ChemComm

Crown ether salt-doped ladder-type conducting polymers for air-stable n-type thermoelectric materials

Journal:	*ChemComm*
Manuscript ID	CC-COM-02-2023-000840.R2
Article Type:	Communication

COMMUNICATION

Crown ether salt-doped ladder-type conducting polymers for air-stable n-type thermoelectric materials

Received 00th January 20xx,
Accepted 00th January 20xx

DOI: 10.1039/x0xx00000x

Ryoto Yura,[a] Shohei Kumagai,[b] Kiyohiro Adachi,[c] Daisuke Hashizume, [c] Toshihiro Okamoto,[b] and Yoshiyuki Nonoguchi*[a]

Thermoelectric energy harvesters based on p- and n-type organic semiconductors are in high demand, while the air stability of n-type devices has long been a challenge. Here, we demonstrate that supramolecular salt-functionalized n-doped ladder-type conducting polymers exhibit excellent stability in the presence of dry air.

Chemical doping is a crucial process for optimizing the thermoelectric properties of organic semiconductors (OSCs)-based materials, where charge injection is enabled by intermolecular charge transfer.[1–5] Thermoelectrics, the direct conversion of temperature difference into electrical voltage and vice versa, has recently attracted considerable interest due to the promise of affordable energy harvesters. Controlled hole (p-type) and electron (n-type) doping techniques are essential to maximise power output and to construct π-type thermoelectric modules. In this sense, it is essential to design suitable doping methods as well as high performance OSCs.

Due to the discovery of polyalkylthiophene, a representative p-type OSC, p-type doping has been well studied to tune their transport properties. State-of-the-art systems for p-doped OSCs include the self-assembled, highly crystalline thienothiophene-based polymer films that impregnate counterbalancing anions into the interspaces/interlayers between tightly packed polymer backbones.[6] In contrast, the development of n-type conducting polymers lags far behind that of p-type conducting polymers. The n-(electron-) doping is, essentially, more difficult than the p-(hole-) doping, due to the high reactivity of carboanions with water and oxygen.[7] In order to achieve improved air stability and efficient transport in n-doped OSCs, molecular design to stabilize the lowest unoccupied molecular orbital (LUMO) of organic semiconductors in combination with high degree conjugation and dense molecular packing has been investigated.[8–10]

Along with the design of n-type OSCs, several n-type dopants have been proposed to improve air-stability, i.e., to enable higher doping efficiencies. In the last two decades, hydride (H^-), hydrogen atom, and radical transfer reactions have been extensively investigated to efficiently inject the electrons into OSCs.[11] In this context, efficient n-dopants include 4-(N,N-dimethylaminophenyl)-N,N-dimethylbenzoimidazole (N-DMBI),[12] and organoruthenium Dimer.[13] Considering redox chemistry, such strategy for molecular doping is universal also for inorganic materials with large specific surface area.[14–18] In turn, various dopants proposed in the inorganic materials field could potentially be applied to n-type OSCs.

Herein we report on air-tolerant n-type doping of OSCs with supramolecular salts, demonstrating comparable air stability to a representative dopant N-DMBI (**Fig. 1**). We use polybenzimidazobenzophenanthroline (BBL), which has a LUMO of 4.0 eV, as a candidate for studying carrier injection.[19,20] The supramolecular salts of crown ethers with potassium hydroxide (KOH), which represent one of the most successful n-doping systems for nanocarbons, [21–26] are used for efficient n-type doping of BBL. Crown ethers are well known to capture alkali metal ions and the mixture of KOH and 18-crown-6-ether (18C6) form their complexes [K^+@18C6]OH^-. The naked anions of hydroxides in the presence of crown ethers can induce electron injection to OSCs, and cationic crown ether-alkali metal ion complexes are expected to counterbalance n-doped (negatively charged) OSCs. This molecular system successfully enables n-type doping of BBLs, and their films exhibit thermoelectric properties comparable to those with reported dopants. Furthermore, we find that BBL films doped with

[a] Faculty of Materials Science and Engineering, Kyoto Institute of Technology, Kyoto 606-8585, Japan.
[b] Material Innovation Research Center (MIRC) and Department of Advanced Materials Science, Graduate School of Frontier Sciences, The University of Tokyo, 5-1-5 Kashiwanoha, Kashiwa, Chiba 277-8561, Japan
[c] RIKEN Center for Emergent Matter Science (CEMS), 2-1 Hirosawa, Wako, Saitama 351-0198, Japan

† Footnotes relating to the title and/or authors should appear here.
Electronic Supplementary Information (ESI) available: Powder X-ray diffraction patters, laser microscopy images, and additional electrical conductivity data. See DOI: 10.1039/x0xx00000x

$[K^+@18C6]OH^-$ exhibit significantly improved stability in both dry air and inert nitrogen (N_2) environments.

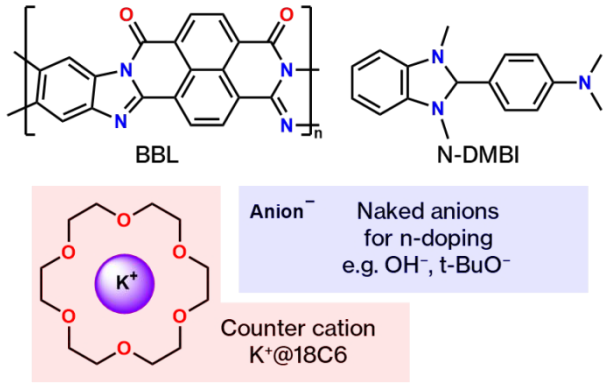

Fig. 1 Chemical structures of BBL, N-DMBI, and supramolecular salts based on crown ethers.

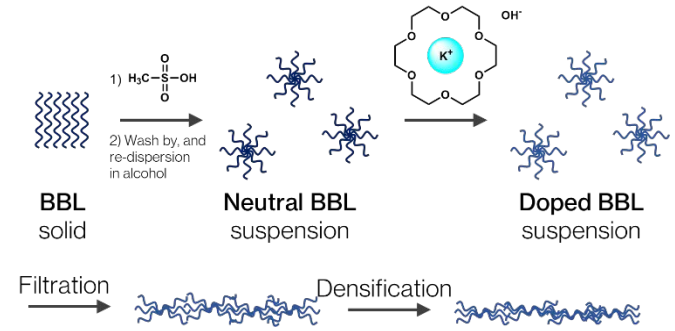

Fig. 2 A brief summary of BBL film preparation in this work.

BBL is known as a relatively air-stable n-type OSC, while it is not easy to prepare its film thick enough to afford low resistivity allowing reliable measurement of thermoelectric properties. Prior to transport study, it is then important to establish a reliable method for preparing robust BBL films. In order to meet this requirement, we filtrated the BBL suspensions prepared by a modified Fabiano's method (**Fig. 2**).[20] Illustratively, this procedure starts with the preparation of a colloidal suspension of BBL by precipitation of BBL dissolved in methanesulfonic acid. After five precipitations in ethanol, the BBL colloids were transferred to dry dimethylformamide (DMF) solution containing 10-100 mM mixture of 18-crown-6-ether and potassium hydroxide.[21] The mixture was heated at 80 °C in a nitrogen atmosphere for 1 hour, followed by vacuum filtration onto PTFE membranes and vacuum drying at 160 °C for 30 minutes. In this process, potassium ions encapsulated in crown ethers are considered as counter cations for reduced BBL. The film colors with and without n-doping were found to be bright gold and brown, respectively (Fig. S1).

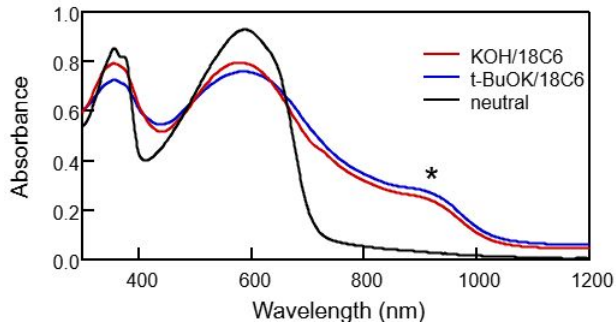

Fig.3 Absorption spectra of BBL suspension in DMF before doping (black), after doping with KOH/18C6 (red) and t-BuOK/18C6 (blue). An asterisk shows the energy transition generated after chemical doping.

The doping progress was monitored using absorption spectroscopy, where absorption spectra provide important information about the electronic structures of solutes. **Fig. 3** shows typical absorption spectra of BBL suspensions before film preparation. After reaction with crown ether complexes with potassium hydroxide as well as butoxide, a new peak developed around 800 nm compared to the neutral BBL suspension. BBL is known to exhibit n-type polaronic absorption around a near-infrared region (approximately 900 nm),[27] suggesting that the present process achieved successful n-type doping of BBL films. Ultraviolet photoelectron yield spectroscopy further revealed the work function shift of 0.5–1.0 eV, before and after treatment with KOH/18-crown ether, supporting the successful n-doping (Fig. S2).

Film preparation conditions and drying temperatures were found to be critical for film quality as assessed by electrical conductivity. For doping efficiency, we chose DMF, where lower electrical conductivity was obtained with other salt-soluble solvents such as 1-butanol. Film roughness was also investigated as it affects conductivity and reproducibility. It was empirically found that the formation of film cracks would be related to the water content in the doping reaction solvents. More importantly, the drying temperature after film filtration was critical for achieving high electrical conductivity, suggesting film preparation with minimal cracking. We also confirmed the crystallinity with and without doping, suggesting the preservation of the molecular stacking of BBL (Fig. S3). Thus, careful treatments are required to prepare applicable, relatively smooth films (Fig. S1) from low thermoplaticity BBL.

The thermoelectric properties of filtrated BBL films have been studied with different dopant concentrations under low pressure N_2, leading to the elucidation of their transport properties. To achieve the best thermoelectric figure of merit: $zT = \frac{S^2\sigma}{\kappa}T$, the electrical conductivity (σ), the Seebeck coefficient (S), and thermal conductivity (κ) must be controlled. In particular, $S^2\sigma$ is referred to the power factor, the measure of power output per unit temperature difference, while both the Seebeck coefficient and the electrical conductivity are significantly modulated by the carrier concentration. Before doping, the film showed extremely high resistivity above $10^7\ \Omega$, which made it difficult to measure reliable thermoelectric properties with our setup. After treatment with supramolecular salts, the films exhibited Seebeck coefficient and electrical conductivity comparable to the literature.[28] The electrical

conductivity increased as a function of molecular dopant concentration by more than two orders of magnitude (**Fig. 4**a), suggesting the controllability of supramolecular salt doping. The Seebeck coefficient decreased as the electrical conductivity increased with doping (Fig. 4b). This S-σ slope would suggest a physical background; the present relationship in the moderate doping region (σ > 0.1 S cm^{-1}) is not inconsistent with the $S \propto \sigma^{-1/4}$ relationship rather than the $S \propto \sigma^{-1}$ relation expected from the Mott's equation. This would correspond to the empirical S-σ relationship for p-type conducting polymer films exhibiting a non-metallic state.[29,30] A peak power factor was estimated to be 1.9 μW m^{-1} K^{-2}. This power factor in the inert N_2 environment is within the range of literature values,[28] further supporting the reliability of our material preparation and measurements.

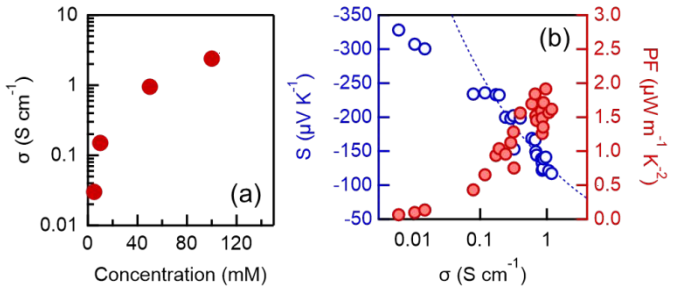

Fig. 4 (a) Electrical conductivity of BBL films depending on dopant concentration for colloid preparation. (b) Seebeck coefficient and power factor dependences on electrical conductivity. The blue dotted line expresses the empirically known $S \propto \sigma^{-1/4}$ relationship.[29] Due to measurement limitation, the electrical conductivity and Seebeck coefficient presented here contain 10% and 15% errors, respectively.

We examined the air-stability of BBL flms functionalized with [K$^+$@18C6]OH$^-$, along with N-DMBI as a standard in the field. We tracked electrical conductivity over time, and analysed its decrease considering a dual exponential function with decay lifetime:

$$\sigma_{normalized} = A_1 \exp\left(-\frac{t}{\tau_1}\right) + A_2 \exp\left(-\frac{t}{\tau_2}\right) \quad (2),$$

where τ_1 and τ_2 are lifetimes, A1 and A2 are the regression coefficients of τ_1 and τ_2, respectively. These lifetimes further yield intensity-weighted average lifetime (τ):

$$\tau = \frac{A_1\tau_1^2 + A_2\tau_2^2}{A_1\tau_1 + A_2\tau_2} \quad (3).$$

Under atmosphere (23 °C, about 50%RH), the supramolecularly doped BBL films developed here showed longer conductivity lifetimes than N-DMBI doped forms by about 45% (**Fig. 5**a and **Table 1**). The lifetime profiles were multi-exponential, and were considered to have at least fast and slow components.

In order to clarify the conspicuous factors for the decays, we examined two environments; first, an inert N_2 environment with a saturated vapor pressure of aqueous NaCl solution (about 75%RH) at room temperature (Fig. S4). This condition allows to study exclusively the effects of water on stability. Another is an aerobic and very dry condition (less than 10%RH), which leads to the assessment of oxygen effects. Looking at the conductivity lifetimes in these conditions (Fig. 5b), we confirmed that the rapid drop in electrical conductivity in the presence of both water and oxygen was improved for dry air or wet N_2 environments, suggesting synergistic oxidative reactions. This trend was also confirmed for n-DMBI doped BBL fil (Fig. S5).

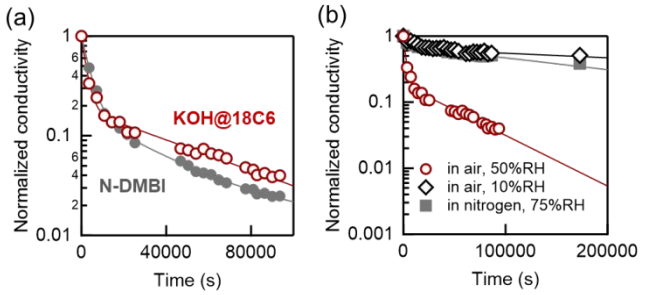

Fig. 5 (a) Conductivity decays for BBL films doped with KOH@18C6 and N-DMBI. (b) Conductivity decay dependences on environments for KOH@18C6-doped BBL films.

Fast lifetime components were attributed to charge neutralization induced by the combination of water and oxygen adsorption on BBL. Kinetic analyses revealed that an initial drop in conductivity occurred with the lifetime of 2-5 × 10^3 seconds, in the high humidity condition (50%RH/air and 75%RH/N_2) while $\tau_1$was much longer in the dry environment. Additionally, this opposite, water-free condition resulted in the significant decrease of the A_1 contribution, and the considerable elongation of the second reaction lifetime (6.4 × 10^5 seconds). As a result, 13-fold increase in the averaged lifetime (6.3 × 10^5 seconds) was achieved compared to the aerobic and humid conditions (4.8 × 10^4 seconds). These results suggest that n-doped organic polymers can potentially be processed for applications without severe degradation.

We have shown that BBL films doped with supramolecular salts [K$^+$@18C6]OH$^-$ exhibit significantly improved stability in the presence of air and water. The sensitivity to air and water revealed in this project suggests appropriate handling of n-type doped OSCs. Our findings also include that the dry air condition is acceptable for processing n-type doped OSCs. So far, the selection of efficient molecular n-type dopants has been limited by severe charge injection such as strong intermolecular charge separation and H$^-$ or H atom transfer reactions. Here we have demonstrated that supramolecular effects such as the naked anion-induced electron transfer can be applied to the n-type doping of OSCs in combination with the consideration of molecular packing and counterbalance after doping. The current route still leaves important issues such as miscibility between polymer side chains and dopants, while recently reported polar systems are likely to be suitable for polar supramolecular systems.[31] The efficient and reliable doping strategy proposed here will provide a basis for the future implementation of air-stable n-type OSCs in electronic and energy devices.

Table 1. Fitting parameters for conductivity decays and their derived, intensity-weighted average decay lifetime.

dopant	condition	A_1	τ_1 (sec)	A_2	τ_2 (sec)	averaged τ (sec)
KOH@18C6	in air, 50%RH	0.82	2.4 × 10^3	0.18	5.7 × 10^4	4.8 × 10^4
	in air, 10%RH	0.34	1.3 × 10^4	0.66	6.4 × 10^5	6.3 × 10^5
	in N_2, 75%RH	0.28	4.9 × 10^3	0.72	2.4 × 10^5	2.4 × 10^5
N-DMBI	in air, 50%RH	0.85	4.0 × 10^3	0.15	4.7 × 10^4	3.3 × 10^4

Y.N. conceived and supervised the project; R.Y. designed and performed the experiments and characterised the compounds; S.K., K.A., D.H. and T.O. conducted X-ray diffraction experiments and their analyses. All the authors wrote the manuscript. T.O. and Y.N. secured financial support.

The authors thank financial support from JST CREST grant number JPMJCR21Q1. Y.N. was awarded MEXT Leading Initiative for Excellent Young Researchers (LEADER). The powder X-ray experiments using synchrotron radiation were performed at the RIKEN Materials Science Beamline (BL44B2) in SPring-8 with the approval of RIKEN (Proposal No. 20210029).

Conflicts of interest

There are no conflicts to declare.

Notes and references

1 O. Bubnova, Z. U. Khan, A. Malti, S. Braun, M. Fahlman, M. Berggren and X. Crispin, *Nat. Mater.*, 2011, **10**, 429–433.
2 M. Sumino, K. Harada, M. Ikeda, S. Tanaka, K. Miyazaki and C. Adachi, *Appl. Phys. Lett.*, 2011, **99**, 093308.
3 Y. Sun, P. Sheng, C. Di, F. Jiao, W. Xu, D. Qiu and D. Zhu, *Adv. Mater.*, 2012, **24**, 932–937.
4 W. Shi, T. Zhao, J. Xi, D. Wang and Z. Shuai, *J. Am. Chem. Soc.*, 2015, **137**, 12929–12938.
5 S. N. Patel, A. M. Glaudell, K. A. Peterson, E. M. Thomas, K. A. O'Hara, E. Lim and M. L. Chabinyc, *Sci Adv*, 2017, **3**, e1700434.
6 Y. Yamashita, J. Tsurumi, M. Ohno, R. Fujimoto, S. Kumagai, T. Kurosawa, T. Okamoto, J. Takeya and S. Watanabe, *Nature*, 2019, **572**, 634–638.
7 D. M. de Leeuw, M. M. J. Simenon, A. R. Brown and R. E. F. Einerhand, *Synth. Met.*, 1997, **87**, 53–59.
8 S. Griggs, A. Marks, H. Bristow and I. McCulloch, *J. Mater. Chem. C*, 2021, **9**, 8099–8128.
9 K. Shi, F. Zhang, C.-A. Di, T.-W. Yan, Y. Zou, X. Zhou, D. Zhu, J.-Y. Wang and J. Pei, *J. Am. Chem. Soc.*, 2015, **137**, 6979–6982.
10 H. Tang, Y. Liang, C. Liu, Z. Hu, Y. Deng, H. Guo, Z. Yu, A. Song, H. Zhao, D. Zhao, Y. Zhang, X. Guo, J. Pei, Y. Ma, Y. Cao and F. Huang, *Nature*, 2022, **611**, 271–277.
11 B. Lüssem, C.-M. Keum, D. Kasemann, B. Naab, Z. Bao and K. Leo, *Chem. Rev.*, 2016, **116**, 13714–13751.
12 P. Wei, J. H. Oh, G. Dong and Z. Bao, *J. Am. Chem. Soc.*, 2010, **132**, 8852–8853.
13 H.-I. Un, S. A. Gregory, S. K. Mohapatra, M. Xiong, E. Longhi, Y. Lu, S. Rigin, S. Jhulki, C.-Y. Yang, T. V. Timofeeva, J.-Y. Wang, S. K. Yee, S. Barlow, S. R. Marder and J. Pei, *Adv. Energy Mater.*, 2019, **9**, 1900817.
14 D. Kiriya, M. Tosun, P. Zhao, J. S. Kang and A. Javey, *J. Am. Chem. Soc.*, 2014, **136**, 7853–7856.
15 Y. Nakashima, R. Yamaguchi, F. Toshimitsu, M. Matsumoto, A. Borah, A. Staykov, M. S. Islam, S. Hayami and T. Fujigaya, *ACS Appl. Nano Mater.*, 2019, **2**, 4703–4710.
16 H. Wang, P. Wei, Y. Li, J. Han, H. R. Lee, B. D. Naab, N. Liu, C. Wang, E. Adijanto, B. C.-K. Tee, S. Morishita, Q. Li, Y. Gao, Y. Cui and Z. Bao, *Proc. Natl. Acad. Sci. U. S. A.*, 2014, **111**, 4776–4781.
17 Q. Hu, Z. Lu, Y. Wang, J. Wang, H. Wang, Z. Wu, G. Lu, H.-L. Zhang and C. Yu, *J. Mater. Chem. A Mater. Energy Sustain.*, 2020, **8**, 13095–13105.
18 A. Tarasov, S. Zhang, M.-Y. Tsai, P. M. Campbell, S. Graham, S. Barlow, S. R. Marder and E. M. Vogel, *Adv. Mater.*, 2015, **27**, 1175–1181.
19 S. Wang, H. Sun, U. Ail, M. Vagin, P. O. Å. Persson, J. W. Andreasen, W. Thiel, M. Berggren, X. Crispin, D. Fazzi and S. Fabiano, *Adv. Mater.*, 2016, **28**, 10764–10771.
20 C.-Y. Yang, M.-A. Stoeckel, T.-P. Ruoko, H.-Y. Wu, X. Liu, N. B. Kolhe, Z. Wu, Y. Puttisong, C. Musumeci, M. Massetti, H. Sun, K. Xu, D. Tu, W. M. Chen, H. Y. Woo, M. Fahlman, S. A. Jenekhe, M. Berggren and S. Fabiano, *Nat. Commun.*, 2021, **12**, 2354.
21 Y. Nonoguchi, M. Nakano, T. Murayama, H. Hagino, S. Hama, K. Miyazaki, R. Matsubara, M. Nakamura and T. Kawai, *Adv. Funct. Mater.*, 2016, **26**, 3021–3028.
22 Y. Nonoguchi, F. Kamikonya, K. Ashiba, K. Ohashi and T. Kawai, *Synth. Met.*, 2017, **225**, 93–97.
23 Y. Nonoguchi, K. Kojiyama and T. Kawai, *J. Mater. Chem. A Mater. Energy Sustain.*, 2018, **6**, 21896–21900.
24 M. Ishimaru, A. Kubo, T. Kawai and Y. Nonoguchi, *MRS Advances*, 2019, **4**, 147–153.
25 H. Ogura, M. Kaneda, Y. Nakanishi, Y. Nonoguchi, J. Pu, M. Ohfuchi, T. Irisawa, H. E. Lim, T. Endo, K. Yanagi, T. Takenobu and Y. Miyata, *Nanoscale*, 2021, **13**, 8784–8789.
26 F. W. Tan, J. Hirotani, Y. Nonoguchi, S. Kishimoto, H. Kataura and Y. Ohno, *Appl. Phys. Express*, 2021, **14**, 045002.
27 K. Xu, H. Sun, T.-P. Ruoko, G. Wang, R. Kroon, N. B. Kolhe, Y. Puttisong, X. Liu, D. Fazzi, K. Shibata, C.-Y. Yang, N. Sun, G. Persson, A. B. Yankovich, E. Olsson, H. Yoshida, W. M. Chen, M. Fahlman, M. Kemerink, S. A. Jenekhe, C. Müller, M. Berggren and S. Fabiano, *Nat. Mater.*, 2020, **19**, 738–744.
28 S. Wang, T.-P. Ruoko, G. Wang, S. Riera-Galindo, S. Hultmark, Y. Puttisong, F. Moro, H. Yan, W. M. Chen, M. Berggren, C. Müller and S. Fabiano, *ACS Appl. Mater. Interfaces*, 2020, **12**, 53003–53011.
29 H. Tanaka, K. Kanahashi, N. Takekoshi, H. Mada, H. Ito, Y. Shimoi, H. Ohta and T. Takenobu, *Sci Adv*, 2020, **6**, eaay8065.
30 A. M. Glaudell, J. E. Cochran, S. N. Patel and M. L. Chabinyc, *Adv. Energy Mater.*, 2015, **5**, 1401072.
31 J. Liu, B. van der Zee, R. Alessandri, S. Sami, J. Dong, M. I. Nugraha, A. J. Barker, S. Rousseva, L. Qiu, X. Qiu, N. Klasen, R. C. Chiechi, D. Baran, M. Caironi, T. D. Anthopoulos, G. Portale, R. W. A. Havenith, S. J. Marrink, J. C. Hummelen and L. J. A. Koster, *Nat. Commun.*, 2020, **11**, 5694.